

# SCIENTIFIC REPORTS

Published online: 05 June 2017

## *Colletotrichum gloeosporioides* ES026

1

2

1

1

1

*Huperzia serrata**Colletotrichum**gloeosporioides* ES026 previously isolated from *H. serrata*  
*de novo**C. gloeosporioides* ES026 to

L-lysine to 5-aminopentanal during HupA biosynthesis. Additionally, we constructed a stable, high-

*CgLDC* *CgCAO**C. gloeosporioides* ES026 in *Escherichia coli*transcription polymerase chain reaction analysis confirmed *CgLDC* *CgCAO**C. gloeosporioides* ES026. These results revealed *CgLDC* and *CgCAO*  
*C. gloeosporioides*

ES026.

Huperzine A (HupA) is a pyridine-type alkaloid derived from *Huperzia serrata*<sup>1,2</sup> and constitutes a highly active acetylcholinesterase inhibitor, making it a valuable therapeutic option for the treatment of Alzheimer's disease (AD)<sup>3,4</sup>. Currently, >46 million people are affected with dementia, with this number predicted to increase to 131.5 million by 2050<sup>5</sup>. HupA is highly selective and exhibits low toxicity, reversibility, and a long duration time relative to other drugs used to treat AD<sup>6</sup>. Furthermore, HupA also exhibits anti-inflammatory activity and appears effective in the treatment of cerebrovascular-type dementia and benign senescent forgetfulness<sup>7,8</sup>.

Currently, HupA is a compound used in herbal supplements mainly extracted from the Chinese club moss *Huperzia serrata*; however, it has a limited distribution and slow growth rate<sup>9</sup>. Furthermore, the complex extraction process from plants and the high costs of downstream purification have impeded HupA utility<sup>10,11</sup>. Consequently, for successful commercial production of HupA, large volumes of *H. serrata* are required. Therefore, in order to protect plant resources from over-harvesting and reduce the cost of HupA-containing medicine, alternative methods for mass producing HupA are needed. The chemical synthesis of HupA was attempted, but the resulting synthesized HupA constituted a racemic mixture exhibiting much less potency than natural HupA. Alternatively,

<sup>1</sup>College of Plant Science and Technology, Huazhong Agricultural University, Wuhan, Hubei, 430070, People's Republic of China. <sup>2</sup>Key Laboratory of Combinatorial Biosynthesis and Drug Discovery (Wuhan University), Ministry of Education, and Wuhan University School of Pharmaceutical Sciences, Wuhan, 430071, People's Republic of China. Correspondence and requests for materials should be addressed to M.W. (email: [wangmo@mail.hzau.edu.cn](mailto:wangmo@mail.hzau.edu.cn))

some endophytic fungi associated with *S. tuberosum* are capable of producing HupA<sup>12–14</sup> with *S. tuberosum* ES026 yielding 45 µg/g dried mycelium according to our previous study<sup>15</sup>. However, HupA production by these endophytes is hindered by low yields and the loss of biosynthetic capability after several generations. Therefore, methods involving overexpression of the enzymes associated with HupA biosynthesis need to be developed in a heterologous host if stable and efficient production is to be achieved<sup>15–17</sup>. Although HupA biosynthesis remains poorly understood, previous studies revealed its initiation by the decarboxylation of L-lysine to generate cadaverine, with the subsequent formation of 5-aminopentanal. Conversion of L-lysine to cadaverine and cadaverine to 5-aminopentanal is catalyzed by lysine decarboxylase (LDC) and

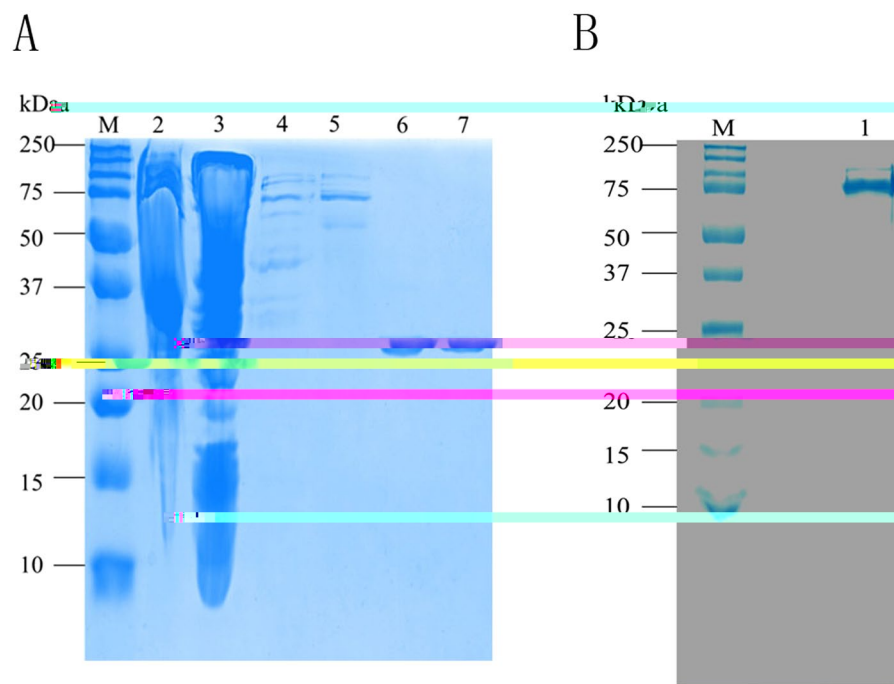


**Fig. 2.** SDS-PAGE analysis of recombinant CgLDC and CgCAO purified by Ni-affinity chromatography. (A) SDS-PAGE analysis of recombinant CgLDC. Molecular mass marker (M), supernatant (lane 2), precipitant (lane 3), cell lysate of BL21 (DE3)-pET28a-CgLDC (lanes 4 and 5), and purified CgLDC (lanes 6 and 7). (B) SDS-PAGE analysis of recombinant CgCAO. Molecular mass marker (M), purified CgCAO (lane 1).

precursor of HupA (Fig. 4). By contrast, no catalytic activity was detected from the inactive forms of CgLDC or CgCAO. These results suggested possible CgLDC and CgCAO involvement in HupA biosynthesis.

**Transformation of *C. gloeosporioides* ES026 and qRT-PCR analysis.** To validate the relationship between *ES026* and *ES026* expression and HupA production, 10 *ES026* and *ES026* overexpressing plasmids containing different promoters were constructed (Fig. 5). According to methods used for *ES026* transformation, *ES026* was transformed using the 10 plasmids, and a randomly selected transformant was confirmed by PCR. Our results indicated amplification of appropriately sized DNA fragments (769 bp and 2072 bp, Fig. 6), verifying *ES026* genetic transformation. Quantification by qRT-PCR of *ES026* and *ES026* expression during fermentation indicated that the *PagdA*-CgLDC and *PalcA*-CgCAO transformants exhibited the highest expression levels (Fig. 7).

To investigate transformant effects on HupA production, HupA yield associated with all mutants was analyzed by LC-HRMS. Our results showed that different expression levels of *ES026* and *ES026* produced different HupA yields; however, high levels of *ES026* and *ES026* expression resulted in higher yields of HupA, although transformants exhibiting the highest expression levels did not produce the highest yields of HupA. Two genetically altered strains (*Polic*-CgLDC and *PgpdA*-CgCAO) yielded stable, high-yielding HupA production (Fig. 8). Our findings revealed that CgLDC and CgCAO were involved in HupA biosynthesis, but that the HupA-synthesis pathway was regulated by separate enzymes.

*ES026* produced a 28-kDa CgLDC protein containing 256 amino acids, with a predicted formula of  $C_{266}H_{444}N_{88}O_{111}S_{23}$ . The theoretical pI of CgLDC was 5.06, and the instability index (II) was 48.51, indicating a potentially unstable protein. *ES026* produced a 76-kDa CgCAO protein containing 672 amino acids, with a predicted formula of  $C_{341}H_{527}N_{92}O_{101}S_{21}$ . The theoretical pI of CgCAO was 5.60, and the instability index (II) was 39.05, indicating a stable protein.

AD affects millions of people worldwide and is among the four principal death-causing diseases, including heart disease, cancer, and stroke. HupA isolated from *ES026* is a natural acetylcholinesterase inhibitor used to treat AD. As mentioned in the introduction, very few biosynthetic studies have been performed with HupA, although no investigations have been reported that have attempted to identify the biosynthetic pathway leading directly to HupA, two enzymes (LDC and CAO) have been proposed as the entry point enzymes into the pathway to the HupA<sup>22, 23</sup>. However, work on that enzymes have only been performed in nonrelated taxa<sup>24</sup>. Nevertheless, the feeding that catalyze key transformations in the biosynthesis of HupA and other Lycopodium alkaloids. In this study, next-generation sequencing and RNA sequencing of *ES026* was performed, and

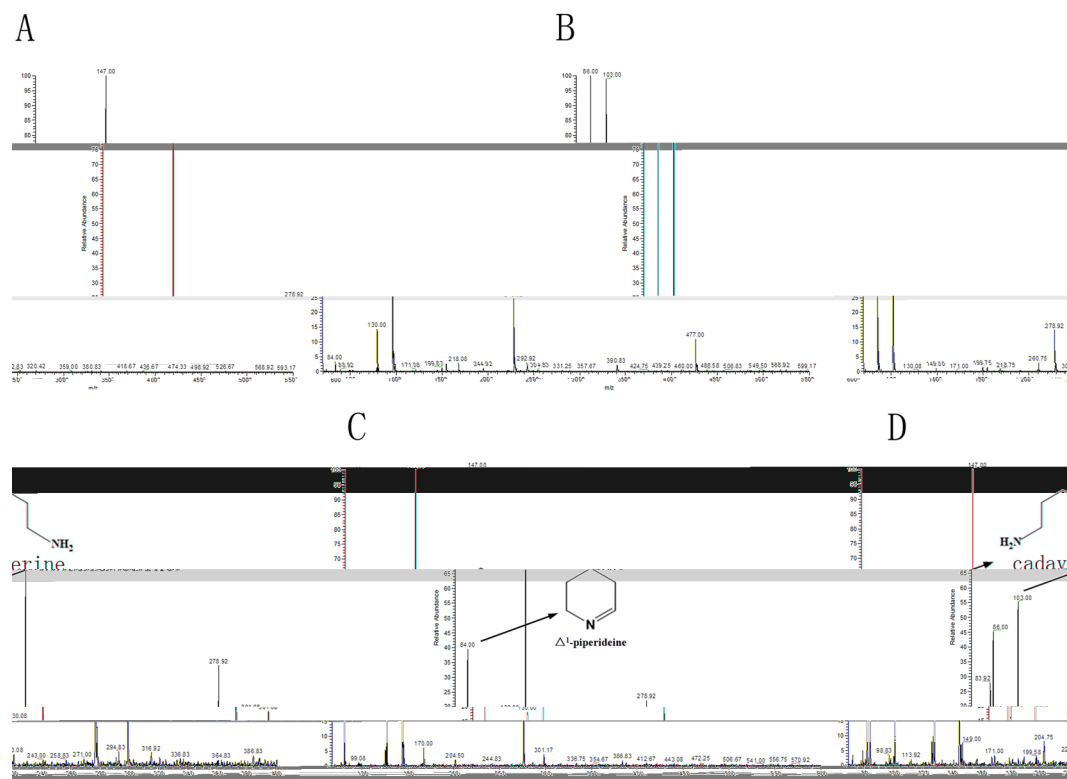


**Fig. 3.** LC-MS analysis of products. (A) LC-MS analysis of L-lysine standard. (B) LC-MS analysis of cadaverine standard. (C) LC-MS analysis of enzymatic formation of cadaverine from L-lysine by CgLDC. Ion chromatograms extracted with  $m/z$  103. (D) LC-MS analysis of enzymatic formation of  $\Delta^1$ -piperidine from cadaverine by CgCAO. Ion chromatograms extracted with  $m/z$  84.

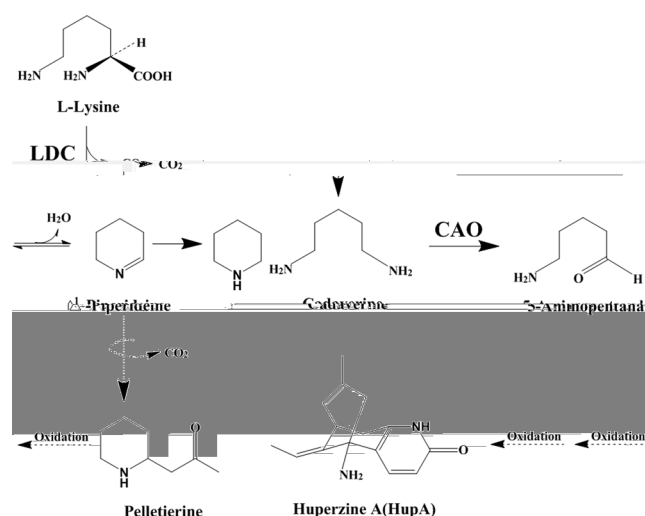


**Fig. 4.** The proposed biosynthetic pathway from L-lysine to  $\Delta^1$ -piperidine. LDC: Lysine decarboxylase; CAO: Copper amine oxidase.

based on transcriptome analyses by Ma <sup>22</sup> and Luo <sup>25, 26</sup>, the HupA biosynthetic pathway was investigated. HupA biosynthesis involves primary and secondary enzyme conversion, initiating with acetyl-CoA and biotin and ending with the development of L-lysine, followed by secondary metabolism involving the development of cadaverine. LDC converts L-lysine to cadaverine, and CAO converts cadaverine to 5-aminopentanal and piperidine. Sun <sup>27</sup> cloned genes from *L. obscurus*, and Du Zhu <sup>28</sup> cloned genes into the endophytic fungus *Aspergillus* sp. Slf14 from *Aspergillus*, enabling verification of specific characteristics related to LDC and CAO biosynthesis of lycopodium alkaloids. Pelletierine, which is a precursor, is also converted, resulting in HupA synthesis. HupA biosynthesis involves LDC as the first enzyme and CAO as the second enzyme, with LDC

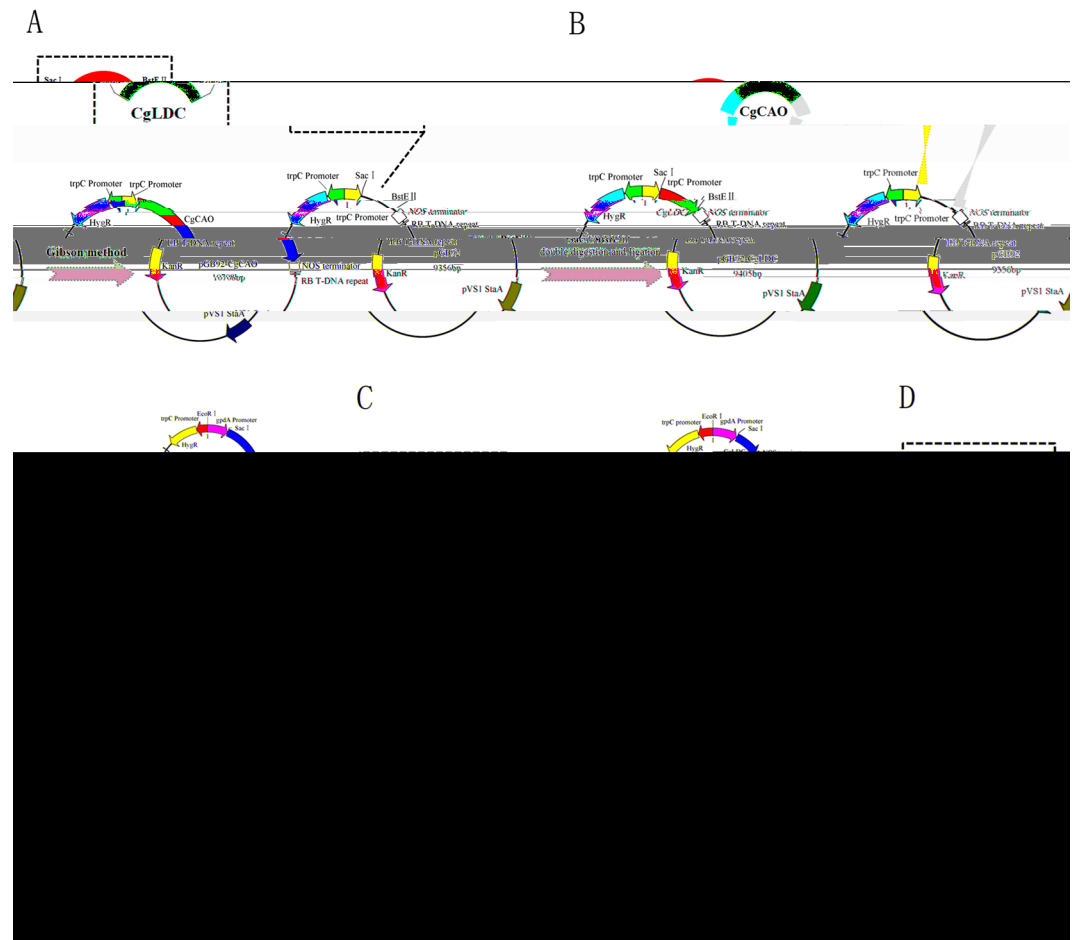


**Fig e5.** Construction of plasmids overexpressing *alcA* and *alcB*. (A) *alcA* was cloned into the pGB92 vector with *trpC* promoter between restriction sites *SacI* and *BstEI* to obtain the recombinant plasmid pGB92-CgLDC. (B) The Gibson method was used to construct the recombinant plasmid pGB92-CgCAO. (C) The *gpdA*, *alcA*, *olic*, and *agdA* promoters were ligated into the recombinant plasmid pGB92-CgLDC to produce pGB93-CgLDC, pGB94-CgLDC, pGB95-CgLDC, and pGB96-CgLDC. (D) The *gpdA*, *alcA*, *olic*, and *agdA* promoters were ligated into the recombinant plasmid pGB92-CgCAO to produce pGB93-CgCAO, pGB94-CgCAO, pGB95-CgCAO, and pGB96-CgCAO.

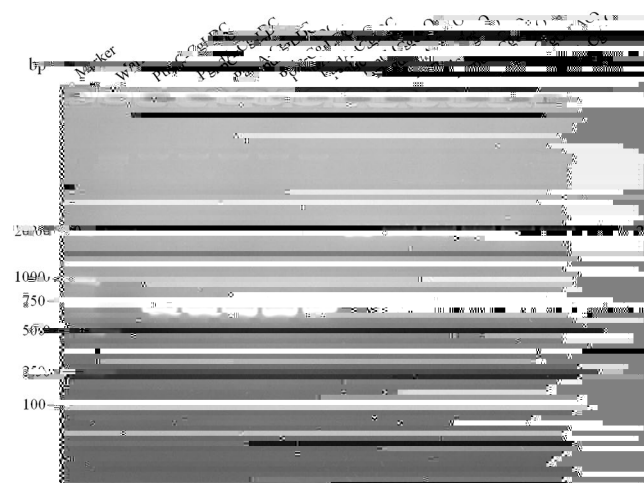


**Fig. e 6.** Identification of transformants by PCR.

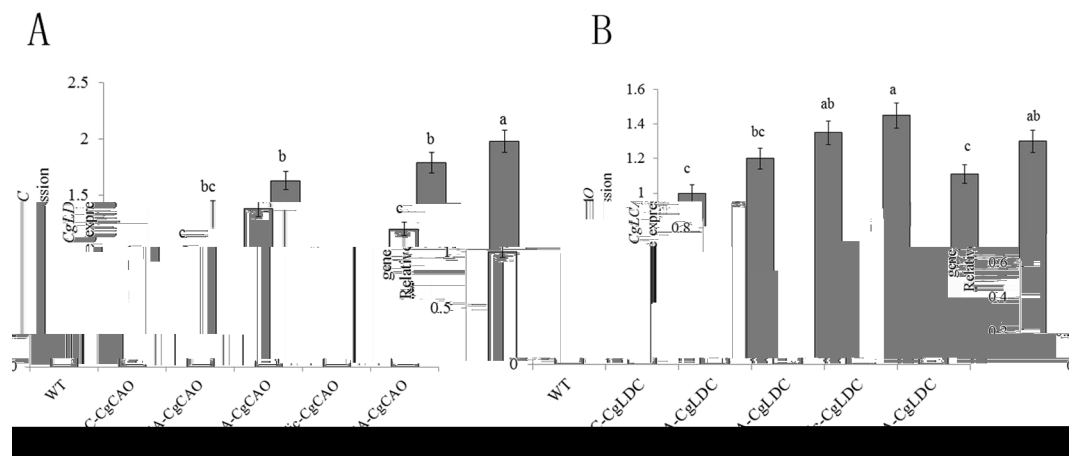


**Fig. 7.** Relative gene expression levels in ES026 and transformed strains. (A) Relative expression of *CgLDC* and *CgCAO* in WT, PtpC-CgCAO, PgpDA-CgCAO, PpalcA-CgCAO, PpolC-CgCAO, and PpagDA-CgCAO transformants using different promoters after 5 days. (B) Relative expression of *CgLDC* and *CgCAO* in WT, PtpC-CgCAO, PgpDA-CgCAO, PpalcA-CgCAO, PpolC-CgCAO, and PpagDA-CgCAO transformants using different promoters after 5 days. \*Duncan's multiple range test;  $p < 0.01$ .

transforming L-lysine to cadaverine, and CAO transforming cadaverine to 5-aminopentanal in lycopodium alkaloid biosynthesis. According to Kyoto Encyclopedia of Genes and Genomes analysis, there is only one pathway involved in synthesizing 5-aminopentanal catalyzed by LDC and CAO.

Recombinant plasmids using different promoters to overexpress *CgLDC* and *CgCAO* in ES026 were constructed, and their expression was determined by qRT-PCR. Additionally, the differential expression of key enzymes involved in HupA biosynthesis and associated metabolic pathways were analyzed, with results indicating that elevated expression of *CgLDC* and *CgCAO* produced increased levels of HupA as compared with wild-type ES026.

In this study, according to the ES026 genome analysis, *CgLDC* and *CgCAO* from ES026 are unique genes, were investigated for their conversion of L-lysine to 5-aminopentanal in HupA biosynthesis. *CgCAO* is different from HsCAO<sup>18</sup>, which can produce 5-aminopentanal. Our results indicated that these enzymes could be efficiently expressed in ES026, that the resulting *CgLDC* was capable of cadaverine production, and the resulting *CgCAO* was capable of 5-aminopentanal production, both of which are HupA biosynthetic intermediates, but this reaction may be weak, experiments are needed to investigate whether *CgLDC* and *CgCAO* have similar properties to other LDCs and CAOs. These findings revealed that genetic modification of ES026 resulted in a variant capable of stable, high-yield production of HupA. Furthermore, we observed that transformants yielding the highest expression of LDC and CAO did not produce the highest yields of HupA, which might have been due to interference by other enzymes involving in HupA biosynthesis. Further investigation is required to elucidate additional details regarding the pathways involved in HupA biosynthesis.

The strain ES026, which produced the highest amount of HupA, was isolated from *ES026* and preserved at the China Center for Type Culture Collection (CCTCC No. 2011046; Wuhan, China). BL21 and DH10B cells were cultured in Luria broth (LB) at 37 °C. The plasmid pET28a containing the kanamycin-resistance gene was used as an assisting plasmid for the transformation of BL21 cells. Plasmids pGB92, pGB93, pGB94, pGB95, and pGB96 containing the hygromycin B resistance were used as assisting plasmids for the transformation of ES026.

**CgLDC and CgCAO** *E. coli* BL21 (DE3) cells and protein purification. According to the ES026 genome sequence and transcriptome analysis<sup>21</sup>, the coding regions of *CgLDC* and *CgCAO* were amplified by polymerase chain reaction (PCR) from ES026 genomic DNA. PCR products were purified using a gel-extraction kit (Omega Bio-tek, Norcross, GA, USA) and cloned into the pET28a vector between the *Nde*I and *Xba*I restriction sites to create plasmids pET28a-CgLDC and pET28a-CgCAO for production and purification of the target proteins. The plasmids expressed recombinant proteins containing a hexahistidine-tag at the C-terminus. Subsequently, pET28a-LDC and pET28a-CAO were transformed into BL21 cells via heat shock, and transformants were verified by PCR and restriction-enzyme digestion.

Cells were cultured to an OD<sub>600</sub> of between 0.6 and 0.8 in LB medium containing 100 µg/mL kanamycin at 37 °C and shaking at 200 rpm. Isopropyl β-D-1-thiogalactopyranoside and CuSO<sub>4</sub> were added to the culture medium to a final concentration of 0.1 mM and 50 µM, respectively, to induce the expression of recombinant *CgLDC* and *CgCAO*. The induced broth was maintained at 16 °C with shaking at 200 rpm for an additional 16 h. Cells were collected by centrifugation at 4 °C at 5000 g for 5 min, resuspended in buffer A [50 mM Tris-HCl, 300 mM NaCl, and 4 mM 2-mercaptoethanol (pH 7.6)], and lysed by sonication. Lysates were then centrifuged

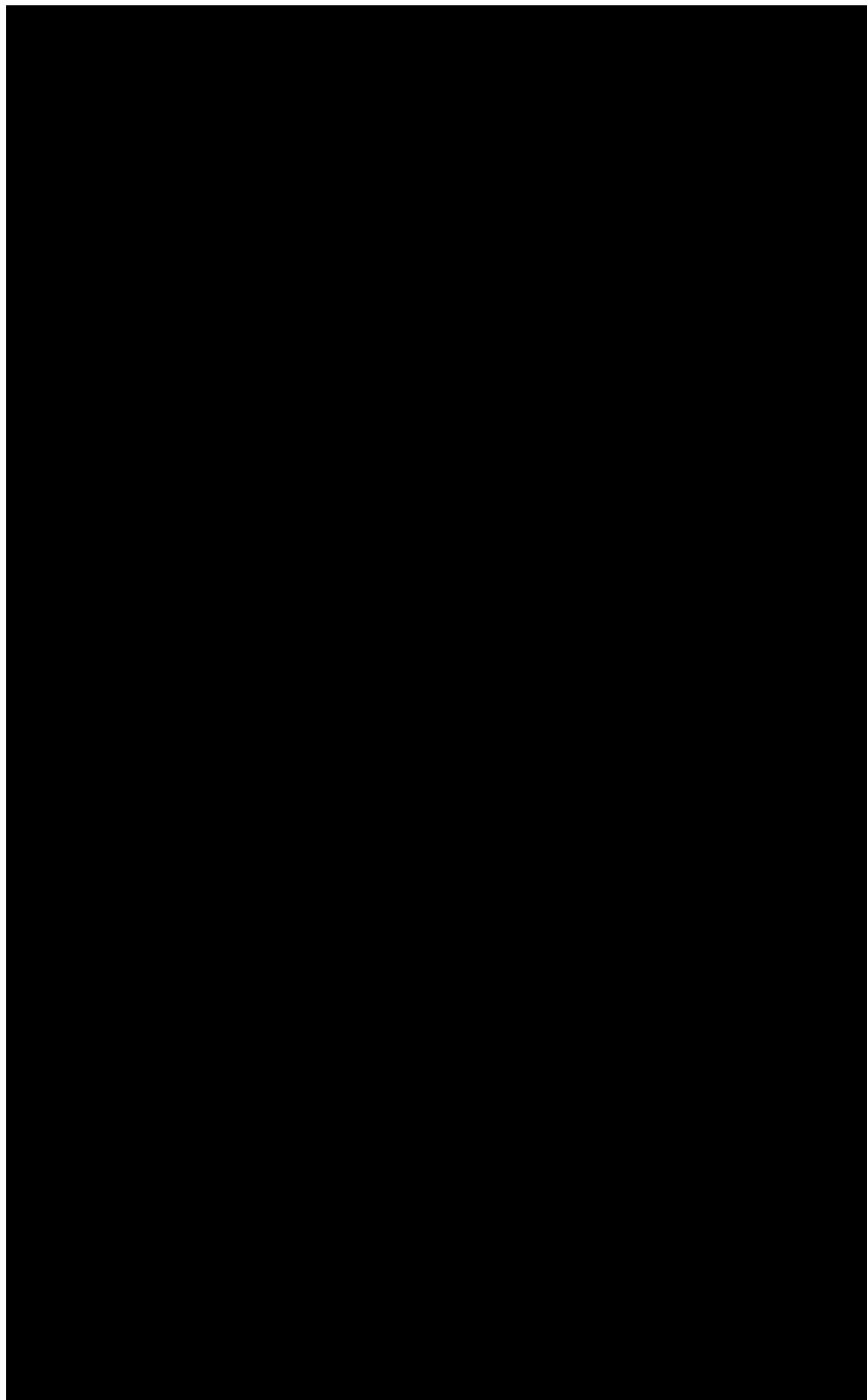


**Figure 8.** HupA yield from ES026 and ES026 transformants. (A) LC-HRMS analysis results of wild-type. (B) LC-HRMS analysis results of HupA yields from wild-type. (C) HupA yields from wild-type. (D) HupA yields from wild-type.

at 12,000 g for 30 min, and the supernatant was loaded onto a Ni-NTA resin column. Recombinant CgLDC and CgCAO proteins were eluted with buffer B [50 mM Tris-HCl, 300 mM NaCl, 4 mM 2-mercaptoethanol, and 500 mM imidazole (pH 7.6)], and the sizes of the purified proteins were analyzed by sodium dodecyl sulfate polyacrylamide gel electrophoresis (SDS-PAGE)<sup>18</sup>.

The CgLDC reaction mixture was prepared according to methods reported by Qiao *et al.*<sup>29</sup>. The reaction contained 1.46 mg L-lysine, 1 mg/mL purified recombinant CgLDC, and 40 µg pyridoxal phosphate in 0.1 mM potassium phosphate buffer (pH 8.0). The mixture was incubated at 37 °C for 45 min prior to adding 30 µL HCl to stop the reaction. The same reaction containing boiled (inactive) CgLDC was used as the negative control. Reaction products were extracted with chloroform and analyzed by liquid chromatography mass spectrometry (LC-MS; Column: Thermo Hypersil GOLD aQ column, 150 mm × 2.1 mm, operation of the mass spectrometer was in electrospray positive ion mode. The MS source and chamber conditions were optimised to give maximum analyte signal intensity as follows: Spray voltage: +3500 V; Capillary Temperature: 320 °C; Sheath Gas: 30.0 psi; Aux Gas: 5.0 psi. Probe Heater Temperature: 300 °C; Scan Range: 50–600 m/z; Scan Rate: 1 Hz), gradient conditions with mobile phases of H<sub>2</sub>O and acetonitrile, both containing 1% acetic acid: 0–2



Transfer of transformant solution was performed according to the method of Zhao<sup>33,34</sup> with minor modifications. Fermented mycelia were collected by centrifugation at 12,000 g or 10 min, followed by drying at 40 °C overnight and grinding into powder. For chemical extraction, each sample of raw material (1 g) was produced using 0.5% HCl [(30 mL (w/v))] overnight, followed by ultrasonication in a water bath at 40 °C for 1 h. The ingredients were then filtered, and the filtrates were rendered with ammonia solution to pH 9.0. After 1 h, the water phase was extracted three times with chloroform, and the combined chloroform extracts were evaporated to dryness. The dry residue was mixed with 1 mL methanol, passed through a 0.45-µm polytetrafluoroethylene syringe filter, and analyzed by LC-HRMS (Agilent Zorbax SB-C18; 150 mm × 4.6 mm, 5-µm diameter, operation of the mass spectrometer (MS) was in electrospray positive ion mode. The MS source and chamber conditions were optimised to give maximum analyte signal intensity as follows: Spray voltage: +3500 V; Capillary Temperature: 320 °C; Sheath Gas: 30.0 psi; Aux Gas: 5.0 psi. Probe Heater Temperature: 300 °C; Scan Range: 50–600 m/z; Scan Rate: 1 Hz). The mobile phases consisted of H<sub>2</sub>O and 5% acetonitrile or 100% acetonitrile (65%: 35%) at a flow rate of 0.6 mL/min. Quantification was performed using the standard curve generated from the HupA standard over a concentration range of between 0.5 and 8.0 mg/L, where the peak area and height showed linear correlations with the absorbance ( $R^2 = 0.9991$ ).

Physicochemical properties were predicted using the ExPASy-ProtParam tool (<http://web.expasy.org/protparam/>), and hydrophobic/hydrophilic analysis was performed by ExPASy-ProtScale (<http://web.expasy.org/protscale/>). Protein signal peptides were predicted using the SignalP 4.1 server (<http://www.cbs.dtu.dk/services/SignalP/>), and transmembrane regions were predicted using the TMHMM server version 2.0 (<http://www.cbs.dtu.dk/services/TMHMM/>). Protein subcellular localization was predicted by ProtComp version 9.0 (<http://linux1.soberberry.com/berry.php?topic=protcompan&group=programs&subgroup=proloc>).

1. Tang, X. C. & Han, Y. F. Pharmacological profile of huperzine A, a novel acetylcholinesterase inhibitor from Chinese herb. *Phytother. Res.* **5**, 281–300, doi:10.1111/cns.1999.5.issue-3 (2010).
2. De Luca, V. & St Pierre, B. The cell and developmental biology of alkaloid biosynthesis. *Phytochem. Rev.* **5**, 168–173, doi:10.1016/S1360-1385(00)01575-2 (2000).
3. Tan, C. & Zhu, D. The progress in the research of Lycopodium alkaloids. *Phytochem. Rev.* **1**, 1–7 (2003).
4. Tang, X. C., He, X. C. & Bai, D. L. Huperzine A: A novel acetylcholinesterase inhibitor. *Phytother. Res.* **24** (1999).
5. Cheng, D. H., Ren, H. & Tang, X. C. Huperzine A, a novel promising acetylcholinesterase inhibitor. *Phytother. Res.* **8**, 97–101, doi:10.1097/00001756-199612200-00020 (1996).
6. McKhann, G. Clinical diagnosis of Alzheimer's disease: report of the NINCDS-ADRDA Work Group under the auspices of Department of Health and Human Services Task Force on Alzheimer's Disease. *Neurology* **34**, 939–944, doi:10.1212/WNL.34.7.939 (1984).
7. Prince, M. & Jackson, Alzheimer's Disease International. *Alzheimer's Disease International* **9**, 5–6 (2015).
8. Liu, G., Kennedy, R. & Greenshields, D. L. Detached and attached Arabidopsis leaf assays reveal distinctive defense responses against hemibiotrophic Colletotrichum spp. *Plant Cell* **20**, 1308–1319, doi:10.1094/MPMI-20-10-1308 (2007).
9. Li, M. Transformation of Coniothyrium minitans, a parasite of Sclerotinia sclerotiorum, with Agrobacterium tumefaciens. *Plant Cell* **24**, 323–329, doi:10.1016/j.femsle.2004.12.033 (2005).
10. Yuan-ming, Sun reaction mixture was prepared according to methods reaction mixture was prepared according to methods Determination of hupzine A in *Phytother. Res.* **33**, 1078–1080 (2002).
11. Xue-wen, Y. I., Zhang, L., Rong-zhen, L. U. O. & Ping, D. U. Study on the Extraction of Huperzine A from Huperzia serrata by Enzymatic Method. *Phytother. Res.* **39**, 19798–19799 (2011).
12. Gong, X. L-Arginine is essential for conidiation in the filamentous fungus Coniothyrium minitans. *Phytother. Res.* **44**, 1368–1379, doi:10.1016/j.fgb.2007.07.007 (2007).
13. Luo, H. Analysis of expressed sequence tags from the Huperzia serrata leaf for gene discovery in the areas of secondary metabolite biosynthesis and development regulation. *Phytother. Res.* **139**, 1–12, doi:10.1111/ppl.2010.139.issue-1 (2010).
14. Luo, H. Comparison of 454-ESTs from Huperzia serrata and Phlegmarius carinatus reveals putative genes involved in lycopodium alkaloid biosynthesis and developmental regulation. *Phytother. Res.* **10**, 1–16, doi:10.1186/1471-2229-10-209 (2010).
15. Zhao, X.-M. Ethanol and Methanol Can Improve Huperzine A Production from Endophytic Colletotrichum gloeosporioides ES026. *Phytother. Res.* **8**, e61777, doi:10.1371/journal.pone.0061777 (2013).
16. Tong, X. T. Miyoshianines A and B, two new Lycopodium alkaloids from Huperzia miyoshiana. *Phytother. Res.* **69**, 576–579, doi:10.1055/s-2003-40648 (2003).
17. Li, W., Zhou, J., Lin, Z. & Hu, Z. Study on fermentation condition for production of huperzine A from endophytic fungus 2F09P03B of Huperzia serrata. *Phytother. Res.* **2**, 254–259 (2007).
18. Sun, J. Y., Morita, H. & Chen, G. S. Molecular cloning and characterization of copper amine oxidase from Huperzia serrata. *Phytother. Res.* **22**, 5784–5790, doi:10.1016/j.bmcl.2012.07.102 (2012).
19. Du, C., Li, J., Tang, Y. T. & Peng, Q. Z. Cloning, prokaryotic expression and characterization of lysine decarboxylase gene from Huperzia serrata. *Phytother. Res.* **30**, 1299–1307 (2014).
20. Ma, X. Q., Tan, C. H. & Zhu, D. Y. A survey of potential huperzine A natural resources in China: Huperziaceae. *Phytother. Res.* **104**, 54–67, doi:10.1016/j.jep.2005.08.042 (2006).
21. Guowei, Z. De Novo RNA Sequencing and Transcriptome Analysis of Colletotrichum gloeosporioides ES026 Reveal Genes Related to Biosynthesis of Huperzine A. *Phytother. Res.* **10**, e012080 (2015).
22. Ma, X. & Gang, D. R. The Lycopodium alkaloids. *Phytother. Res.* **21**(6), 752–772, doi:10.1039/b409720n (2004).
23. Hemscheidt, T. Tropane and Related Alkaloids. *Phytother. Res.* **175**–206 (2000).
24. Gerdes, H. J. & Leistner, E. Stereochemistry of reactions catalyzed by L-lysine decarboxylase and diamine oxidase. *Phytother. Res.* **18**, 771–775, doi:10.1016/0031-9422(79)80011-4 (1979).
25. Ma, X. Huperzine A from Huperzia species—an ethnopharmacological review. *Phytother. Res.* **113**, 15–344, doi:10.1016/j.jep.2007.05.030 (2007).
26. Chen, S. 454 EST analysis detects genes putatively involved in ginsenoside biosynthesis in *Phytother. Res.* **30**, 1593–1601, doi:10.1007/s00299-011-1070-6 (2011).
27. Moller, S. G. & Mcpherson, M. J. Molecular and functional studies of copper amine oxidase from Arabidopsis thaliana. *Phytother. Res.* **23**, 630s–630S, doi:10.1042/bst023630s (1995).

28. Zhu, D. . . . A novel endophytic Huperzine A-producing fungus, *Shiraia* sp. Slf14, isolated from *Huperzia serrata*. . . . . **109**, 1469–1478, doi:[10.1111/jam.2010.109.issue-4](https://doi.org/10.1111/jam.2010.109.issue-4) (2010).
29. Changsheng, Q. . . . A method for assay of the activity of L-lysine Decarboxylase. . . . . **27**, 189–192 (2013).
30. Gibson Method (Dictionary Geotechnical Engineering/wörterbuch Geotechnik). 606–606 (2006).
31. Bitsadze, N., Siebold, M., Koopmann, B. & Tiedemann, A. Single and combined colonization of *Sclerotinia sclerotiorum* sclerotia by the fungal mycoparasites *Coniothyrium minitans* and *Microsphaeropsis ochracea*. . . . . **64**, 690–700, doi:[10.1111/ppa.12302](https://doi.org/10.1111/ppa.12302) (2015).
32. Frandsen, R. J. A guide to binary vectors and strategies for targeted genome modification in fungi using *Agrobacterium tumefaciens*-mediated transformation. . . . . **87**, 247–262, doi:[10.1016/j.mimet.2011.09.004](https://doi.org/10.1016/j.mimet.2011.09.004) (2011).
33. Venugopalan, A. & Srivastava, S. Enhanced camptothecin production by ethanol addition in the suspension culture of the endophyte, *Fusarium solani*. . . . . **188**, 251–7, doi:[10.1016/j.biortech.2014.12.106](https://doi.org/10.1016/j.biortech.2014.12.106) (2015).
34. Koyanagi, T., Matsumura, K., Kuroda, S. & Tanizawa, K. Molecular Cloning and Heterologous Expression of Pea Seedling Copper Amine Oxidase. . . . . **64**, 717–722, doi:[10.1271/bbb.64.717](https://doi.org/10.1271/bbb.64.717) (2000).

is work was supported by the Ministry of Science and Technology of the People's Republic of China [the Project of International scientific and technological cooperation between China and South Korea (Grant No. 2011DFA31290)] and thanks are due to professor Tiangang Liu (Wuhan University) for assistance with the experiments and valuable discussion.

Mo Wang and Xiangmei Zhang conceived and designed the experiments. Xiangmei Zhang and Zhangqian Wang performed the experiments. Xiangmei Zhang and Qian Yang analyzed the data. Xiangmei Zhang and Saad Jan wrote the manuscript. All authors have read and approved the manuscript for publication.

**Competing interests:** The authors declare that they have no competing interests.

**Publisher's note:** Springer Nature remains neutral with regard to jurisdictional claims in published maps and institutional affiliations.



**Open Access** This article is licensed under a Creative Commons Attribution 4.0 International License, which permits use, sharing, adaptation, distribution and reproduction in any medium or format, as long as you give appropriate credit to the original author(s) and the source, provide a link to the Creative Commons license, and indicate if changes were made. The images or other third party material in this article are included in the article's Creative Commons license, unless indicated otherwise in a credit line to the material. If material is not included in the article's Creative Commons license and your intended use is not permitted by statutory regulation or exceeds the permitted use, you will need to obtain permission directly from the copyright holder. To view a copy of this license, visit <http://creativecommons.org/licenses/by/4.0/>.

© The Author(s) 2017